Imaging of the Osteoporotic Spine – Quantitative Approaches in Diagnostics and for the Prediction of the Individual Fracture Risk

Bildgebung der osteoporotischen Wirbelsäule – quantitative Ansätze für die Diagnostik und Abschätzung des individuellen Frakturrisikos

Authors

Nico Sollmann[1, 2, 3, 4], Jan Stefan Kirschke[3, 4], Sophia Kronthaler[5], Christof Boehm[5], Michael Dieckmeyer[3], Daniel Vogele[1], Christopher Kloth[1], Christoph Gerhard Lisson[1], Julio Carballido-Gamio[6], Thomas Marc Link[2], Dimitrios Charalampos Karampinos[5], Subburaj Karupppasamy[7, 8], Meinrad Beer[1], Roland Krug[2], Thomas Baum[3]

Affiliations

1 Department of Diagnostic and Interventional Radiology, University Hospital Ulm, Ulm, Germany
2 Department of Radiology and Biomedical Imaging, University of California San Francisco, San Francisco, CA, United States
3 Department of Diagnostic and Interventional Neuroradiology, Klinikum rechts der Isar, Technical University of Munich, Munich, Germany
4 TUM-Neuroimaging Center, Klinikum rechts der Isar, Technical University of Munich, Munich, Germany
5 Department of Diagnostic and Interventional Radiology, Klinikum rechts der Isar, Technical University of Munich, Munich, Germany
6 Department of Radiology, University of Colorado – Anschutz Medical Campus, Aurora, CO, United States
7 Engineering Product Development (EPD) Pillar, Singapore University of Technology and Design, Singapore
8 Sobey School of Business, Saint Mary's University, Halifax, NS, Canada

Correspondence

Dr. Nico Sollmann
Department of Diagnostic and Interventional Radiology, University Hospital Ulm, Albert-Einstein-Allee 23, 89081 Ulm, Germany
Tel.: +49/7 31/50 06 10 01
nico.sollmann@tum.de

Key words

bone mineral density, computed tomography, magnetic resonance imaging, proton density fat fraction, quantitative imaging, vertebral fracture

received 02.09.2021
accepted 03.02.2022
published online 11.05.2022

Bibliography

Fortschr Röntgenstr 2022; 194: 1088–1099
DOI 10.1055/a-1770-4626
ISSN 1438-9029

Georg Thieme Verlag KG, Rüdigerstraße 14, 70469 Stuttgart, Germany

ABSTRACT

Osteoporosis is a highly prevalent systemic skeletal disease that is characterized by low bone mass and microarchitectural bone deterioration. It predisposes to fragility fractures that can occur at various sites of the skeleton, but vertebral fractures (VFs) have been shown to be particularly common. Prevention strategies and timely intervention depend on reliable diagnosis and prediction of the individual fracture risk, and dual-energy X-ray absorptiometry (DXA) has been the reference standard for decades. Yet, DXA has its inherent limitations, and other techniques have shown potential as viable add-on or even stand-alone options. Specifically, three-dimensional (3 D) imaging modalities, such as computed tomography (CT) and magnetic resonance imaging (MRI), are playing an increasing role. For CT, recent advances in medical image analysis now allow automatic vertebral segmentation and value extraction from single vertebral bodies using a deep-learning-based architecture that can be implemented in clinical practice. Regarding MRI, a variety of methods have been developed over recent years, including magnetic resonance spectroscopy (MRS) and chemical shift encoding-based water-fat MRI (CSE-MRI) that enable the extraction of a vertebral body's proton density fat fraction (PDFF) as a promising surrogate biomarker of bone health. Yet, imaging data from CT or MRI may be more efficiently used when combined with advanced analysis techniques such as texture analysis (TA; to provide spatially resolved assessments of vertebral body composition) or finite element analysis (FEA; to provide estimates of bone strength) to further improve fracture prediction. However, distinct and experimentally validated diagnostic criteria for osteoporosis based on CT- and MRI-derived meas-

ures have not yet been achieved, limiting broad transfer to clinical practice for these novel approaches.

Key Points:

- DXA is the reference standard for diagnosis and fracture prediction in osteoporosis, but it has important limitations.
- CT- and MRI-based methods are increasingly used as (opportunistic) approaches.
- For CT, particularly deep-learning-based automatic vertebral segmentation and value extraction seem promising.
- For MRI, multiple techniques including spectroscopy and chemical shift imaging are available to extract fat fractions.
- Texture and finite element analyses can provide additional measures for vertebral body composition and bone strength.

Citation Format

- Sollmann N, Kirschke JS, Kronthaler S et al. Imaging of the Osteoporotic Spine – Quantitative Approaches in Diagnostics and for the Prediction of the Individual Fracture Risk. Fortschr Röntgenstr 2022; 194: 1088–1099

ZUSAMMENFASSUNG

Osteoporose ist eine systemische Skeletterkrankung mit sehr hoher Prävalenz, die durch verminderte Knochensubstanz und mikrostrukturelle Verschlechterung des Knochens gekennzeichnet ist. Osteoporose prädisponiert zu Frakturen, welche an verschiedenen Stellen des Skeletts auftreten können, wobei hierunter Wirbelkörper-Frakturen besonders häufig sind. Präventionsmaßnahmen sowie rechtzeitige Interventionen basieren auf einer zuverlässigen Diagnose sowie einer Abschätzung des individuellen Frakturrisikos, wobei die Doppelröntgen-Absorptiometrie (DXA) seit Jahrzehnten als Referenzstandard gilt. Die DXA-Methode hat jedoch inhärente Limitationen, während andere Techniken ein hohes Potenzial als praktikable ergänzende oder sogar alleinige Alternativen gezeigt haben. Im Speziellen spielen dreidimensionale (3 D) Modalitäten der Bildgebung, wie die Computertomografie (CT) und die Magnetresonanztomografie (MRT), eine zunehmend wichtige Rolle. In Bezug auf die CT erlauben aktuelle Entwicklungen aus dem Bereich der medizinischen Bildanalyse inzwischen eine automatisierte Segmentierung und Extraktion relevanter Maßzahlen einzelner Wirbelkörper unter Verwendung von „Deep-Learning"-Algorithmen, welche in die klinische Praxis implementiert werden können. In Bezug auf die MRT stehen dank der Entwicklungen über die letzten Jahre eine Vielzahl an Methoden zur Verfügung, insbesondere die Magnetresonanzspektroskopie (MRS) sowie die Bildgebung mittels „Chemical Shift Enconding-Based" Wasser-Fett-Differenzierung zur Gewinnung der „Proton Density Fat Fraction" (PDFF) eines Wirbelkörpers als vielversprechendem Surrogatmarker der Knochengesundheit. Bildgebungsdaten der CT oder MRT könnten jedoch noch effizienter genutzt werden durch eine Kombination mit fortschrittlichen Analyse-Techniken, wie beispielsweise Texturanalyse (TA; zur räumlich hoch aufgelösten Auswertung des Wirbelkörperaufbaus) oder Finite-Elemente-Analyse (FEA; zur Abschätzung der Knochenstärke) zur weiteren Verbesserung der Frakturvorhersage. Bisweilen konnten jedoch noch keine spezifischen und experimentell validierten Diagnosekriterien für die Osteoporose anhand CT- und MRT-basierter Parameter etabliert werden, was die breitere Translation in die klinische Praxis für diese neuen Ansätze erschwert.

Kernaussagen:

- Die DXA-Methode stellt den Referenzstandard für die Diagnose und Frakturabschätzung bei Osteoporose dar, hat jedoch wichtige Limitationen.
- CT- und MRT-basierte Techniken werden zunehmend im Rahmen (opportunistischer) Ansätze genutzt.
- In Bezug auf die CT ist insbesondere die „Deep-Learning"-basierte automatische Wirbelkörpersegmentierung mit Extraktion von Maßzahlen bedeutsam.
- Für die MRT stehen vielfältige Techniken inklusive der Spektroskopie und der „Chemical-Shift"-Bildgebung zur Extraktion der „Fat Fraction" zur Verfügung.
- Textur- und Finite-Elemente-Analysen können eine zusätzliche Bestimmung des Wirbelkörper-Aufbaus und der Knochenstärke ermöglichen.

Introduction

Osteoporosis is characterized by low bone mass and microarchitectural bone deterioration [1]. Osteoporotic fragility fractures have a major impact on quality of life and are associated with premature mortality [2, 3]. While fragility fractures can occur at various sites of the skeleton, vertebral fractures (VFs) are prevalent in osteoporosis [1]. The clinical problem is that osteoporotic VFs occur frequently but often stay asymptomatic, thus delaying treatment initiation and prevention of future additional fractures [4].

The major aims of osteoporosis treatment are fracture prevention and therapy of fracture-related complications [1]. Effective prevention strategies are linked to the reliable assessment of the individual patient's fracture risk, with dual-energy X-ray absorptiometry (DXA) being the reference standard for decades [1]. However, DXA has considerable inherent limitations that impede its clinical value: DXA can be inaccurate in differentiating between patients with and without prevalent VFs, in predicting new fragility fractures, and for therapy monitoring [5–7]. Consequently, there is a need for alternatives to DXA-based measurements of areal bone mineral density (aBMD) to improve the diagnosis and prediction of individual fracture risk, which include computed tomography (CT) and magnetic resonance imaging (MRI) together with advanced image analysis techniques.

The purpose of this review article is to provide an overview of quantitative approaches to image and evaluate the osteoporotic spine. We herein discuss current as well as emerging quantitative

approaches including their respective methodological principles, important caveats and perspectives, and advances in image-based analysis techniques. Relevant studies were identified by PubMed search (http://www.ncbi.nlm.nih.gov/pubmed).

Overview of methods and findings

Dual-energy X-ray absorptiometry

As a two-dimensional (2 D) densitometry method, DXA can provide quantitative measures such as bone area, bone mineral content, and aBMD (▶ **Fig. 1**). DXA represents the reference method to diagnose osteoporosis and estimate fracture risk, with a DXA-derived T-score of ≤-2.5 defining osteoporosis according to the World Health Organization (WHO) [8]. Yet, a main limitation of DXA is its 2 D character, making the technique prone to bias due to several factors such as vertebral size, patient positioning, and degenerative joint disease that cannot be resolved within the simple 2 D planar projections [9–11].

Since 2007, it has been acknowledged by the WHO that the DXA-derived T-score is not sufficient as the stand-alone criterion to identify patients at high fracture risk eligible for intervention [12]. The trabecular bone score (TBS) has been developed to expand the utility of DXA beyond conventional aBMD measurements as an attempt to increase clinical value. In essence, TBS is based on gray-level texture analysis (TA) of 2 D data from DXA and provides an indirect index for trabecular microstructure [13]. Specifically, TBS has been shown to predict fracture risk independently of aBMD in postmenopausal women [13]. While the actual accuracy of fracture risk prediction is only slightly increased by spine TBS when compared to aBMD measurements, a low TBS is relevant to correct identification of osteopenic women at high fracture risk, hence providing opportunities for improved clinical management [14]. Clinical feasibility is supported by the availability of TBS as a modifier in the Fracture Risk Assessment Tool (FRAX®; http://www.sheffield.ac.uk/FRAX/), a widely used computer-based algorithm that integrates clinical risk factors (alone or in combination with aBMD) to calculate the 10-year probability to sustain an osteoporotic fracture [15].

Computed tomography

Principles and main findings

In contrast to DXA, CT enables the extraction of volumetric BMD (vBMD) since it is a three-dimensional (3 D) imaging modality. However, there are no official diagnostic criteria for the diagnosis of osteoporosis based on CT data, given that the WHO definition of osteoporosis relates to DXA [8]. Yet, the American College of Radiology established reference values to allow the use of CT data for standardized diagnosis in osteoporosis: vBMD < 80 mg/cm^3 is defined as osteoporosis and 80 ≤ vBMD ≤ 120 mg/cm^3 is defined as osteopenia for the lumbar spine [16]. Importantly, the vBMD values for this categorization relate to measurements within trabecular bone tissue (trabecular vBMD), which is the anisotropic, porous, and heterogeneous material within a vertebral body [16, 17].

Conventionally, quantitative CT (QCT) refers to a dedicated CT scan for vBMD assessment, with the acquisition being combined with the application of software packages to calculate the vBMD that is typically derived from three vertebral levels (e. g., vertebral bodies L1 to L3) (▶ **Fig. 2**) [18, 19]. Commonly, this is achieved with measurements in a reference phantom with known density during the same scanning session to be able to convert attenuation values in Hounsfield units (HU) to vBMD [18, 19]. A fundamentally different approach is to use routine CT data acquired for other clinical purposes than osteoporosis assessment (e. g., oncologic staging) for measurements of vBMD, which is referred to as opportunistic CT [18, 19]. Apparently, such opportunistically used routine CT data may have been acquired without a reference phantom, and a major benefit of opportunistic CT is that it can save additional scanning by conventional QCT for vBMD assessments. While dedicated QCT imaging with software and phantom imaging has been used even prior to DXA, opportunistic CT has received increased attention in recent years [18, 19]. This importance seems related to osteoporosis screening benefits in patients who undergo regular CT exams and have an increased risk for osteoporosis due to comorbidity or treatment side effects, as is the case for many oncologic patients [20].

Regarding opportunistic CT, early work in 2000 has shown that by applying a conversion equation, bone densitometry is feasible for clinical non-contrast as well as contrast-enhanced CT scans, demonstrating non-significant differences in vBMD between QCT and opportunistically used CT data [21]. Other work demonstrated that discrimination between patients with and without VFs was possible, and that correlations between vBMD measurements obtained from opportunistically used CT and QCT have been highly significant both in-vitro and in-vivo in oncologic patients [22]. A multitude of studies have shown comparable findings of lower vBMD values in patients with VFs for opportunistically used CT, with varying but overall acceptable discriminatory power to differentiate between patients with and without such fractures [23–25]. Furthermore, a vBMD cutoff of 90 mg/cm^3 and 145 mg/cm^3 derived from opportunistically used CT showed a sensitivity/specificity of 100 %/63.8 % and 100 %/57 % for DXA-defined osteoporosis and osteopenia, respectively [26, 27]. However, these values may not be regarded as absolute, likely being subject to some degree of variation related to CT system hardware and software characteristics, vendor-specific differences, and respective HU-to-BMD conversion equations.

Potential caveats

While vBMD measurements in CT data are increasingly accepted in the clinical routine for opportunistic osteoporosis assessment, the approach comes with important caveats. Opportunistic assessment implies that both non-contrast and contrast-enhanced image data may be present. Yet, contrast media can drastically change attenuation within vertebral bone, which is due to its high vascularization [28]. Recently, it has been reported that the increase in vBMD values related to trabecular bone contrast perfusion could reach a plateau at approximately 7–9 %, which may be irrespective of the exact contrast phase and would make it comparatively easy to correct for [29, 30]. However,

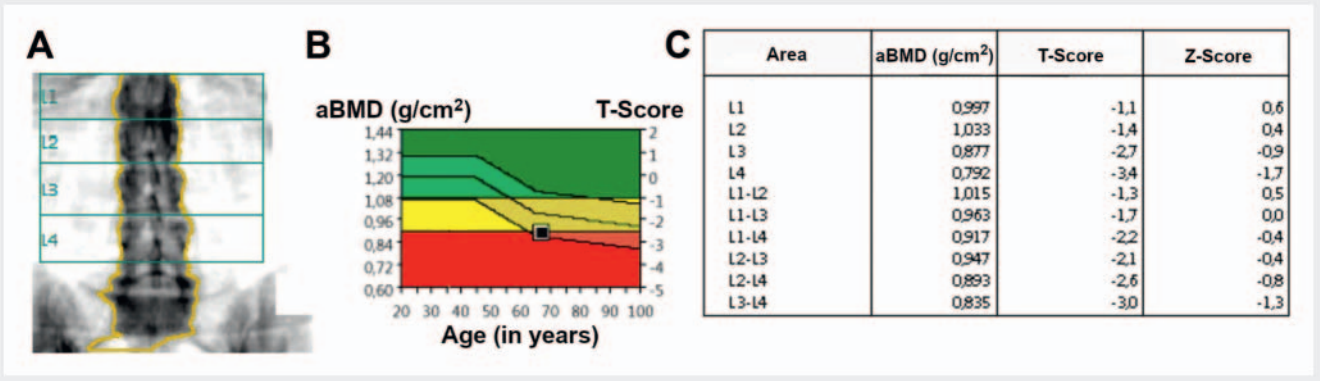

Area	aBMD (g/cm²)	T-Score	Z-Score
L1	0,997	-1,1	0,6
L2	1,033	-1,4	0,4
L3	0,877	-2,7	-0,9
L4	0,792	-3,4	-1,7
L1-L2	1,015	-1,3	0,5
L1-L3	0,963	-1,7	0,0
L1-L4	0,917	-2,2	-0,4
L2-L3	0,947	-2,1	-0,4
L2-L4	0,893	-2,6	-0,8
L3-L4	0,835	-3,0	-1,3

▶ **Fig. 1** Dual-energy X-ray absorptiometry (DXA). Placement of the regions of interest and measurement of areal bone mineral density (aBMD) at the lumbar spine (L1-L4) using DXA. **A** Coronal overview of the lumbar spine with identification of spinal levels of interest; **B** graphical illustration of aBMD values and T-scores in relation to an age- and gender-matched reference cohort (green area: normal values; yellow area: osteopenic range; red: osteoporotic range); **C** area-wise listing of aBMD values as well as Z- and T-scores. The Z-score compares individual BMD to the average value of a cohort with the same age and gender, while the T-score reflects how much individual BMD differs from that of an average healthy 30-year-old adult.

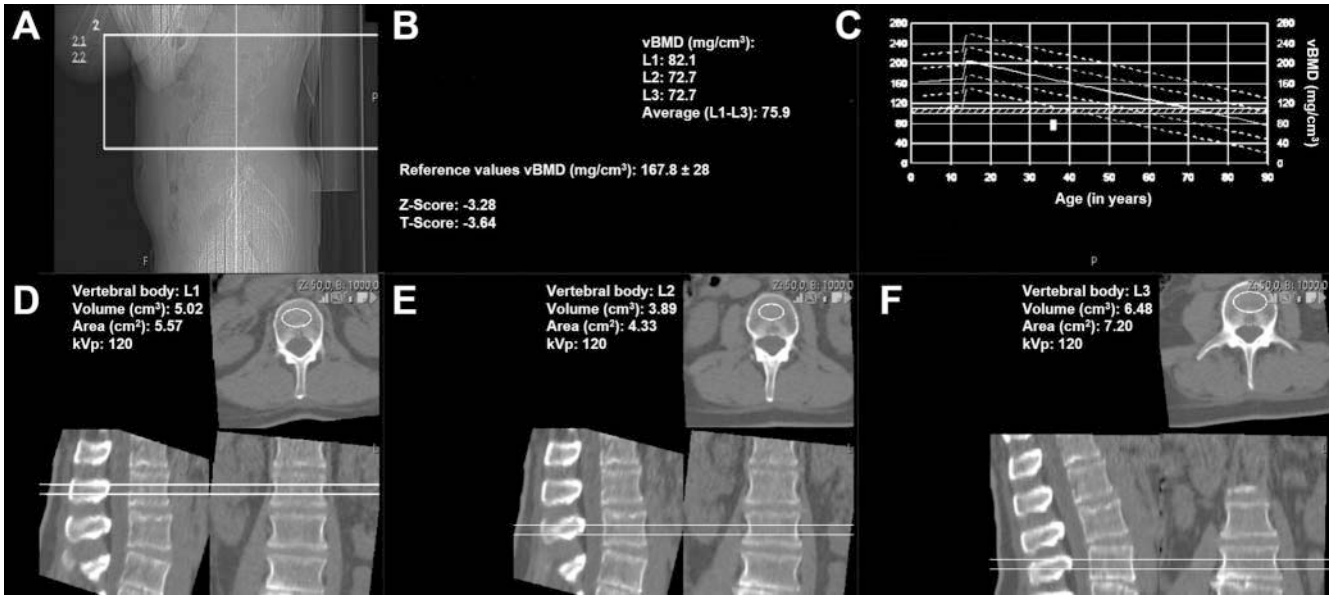

▶ **Fig. 2** Quantitative computed tomography (QCT). Placement of regions of interest and measurement of volumetric bone mineral density (vBMD) at the lumbar spine (L1-L3) using QCT (with standard software and related measurements in a reference phantom with known density for conversion of attenuation values in Hounsfield units [HU] to vBMD). **A** Initial sagittal survey scan to identify suitable vertebral bodies for placement of the regions of interest; **B** vBMD values for three vertebral levels (L1-L3) and average vBMD, together with corresponding vBMD reference values derived from a reference cohort and Z- and T-scores; **C** graphical illustration of vBMD values in relation to an age- and gender-matched reference cohort; **D** placement of the region of interest within L1; **E** placement of the region of interest within L2; **F** placement of the region of interest within L3. Osteoporosis is typically characterized by decreased vBMD. The Z-score compares individual BMD to the average value of a cohort with the same age and gender, while the T-score reflects how much individual BMD differs from that of an average healthy 30-year-old adult.

universal correction for contrast-enhanced CT has not been achieved and is the subject of ongoing research, with many factors influencing attenuation values such as contrast phase and volume of injected contrast medium, heart ejection fraction, and extent of vascularization [18, 19]. Whenever CT data is used opportunistically for osteoporosis diagnostics, caution is needed if a contrast agent was used, indicating that sufficient adjustment of HU-to-BMD conversion equations needs to be achieved.

Furthermore, calibration can become an issue, given that routine CT is not standardly performed with reference phantoms, unlike in the case of dedicated QCT exams with simultaneous phantom measurements (i. e., synchronous calibration). Hence, calibration in the opportunistic setup has to be achieved by separate phantom scans (i. e., asynchronous calibration) or should be guaranteed by internal calibration that considers known densities of body tissues captured by the scan as references [18, 19]. Particularly for asynchronous calibration, the quality of opportunistically used data must be ensured to establish accurate HU-to-BMD conversion equations.

Of note, the radiation dose applied during CT to obtain images with high quality and sufficient spatial resolution is substantial, with dose values in the order of ~3 mSv for high-resolution CT compared to 0.001–0.05 mSv for DXA or 0.06–0.3 mSv for conventional QCT at the spine [19, 31]. When CT is exclusively acquired for clinical purposes (e. g., oncologic staging), indication for CT is justified, and its opportunistic use could save additional dedicated examinations for osteoporosis evaluation, thus restricting the overall radiation exposure of the patient.

Perspectives and novel analysis approaches

Recent methodological advances may soon compensate for aspects of calibration and radiation exposure issues. In this regard, dual-energy CT (DECT) systems that have become commercially available in recent years may facilitate extraction of vBMD values from routine data, given that they do not only operate with monoenergetic images as conventional CT does. Thus, using DECT can foster vBMD extraction without the need for dedicated phantom-based calibration, showing strong correlations with QCT ex-vivo as well as with DXA measurements in a phantom study [32, 33]. In vivo, vBMD measurements from DECT and QCT showed excellent correlations, and conversion with adjustment for individual vessel iodine concentrations also enabled high correlations between vBMD of non-contrast and contrast-enhanced DECT [34, 35]. Considering radiation safety, however, it should be noted that DECT is related to higher exposures than conventional CT, but radiation dose savings could be possible if virtual non-contrast images replace additional dedicated non-contrast scanning. For multi-detector CT systems that are still more widely used and more affordable, radiation dose reduction for spine imaging seems feasible when alternative schemes are implemented, such as sparse sampling that has shown high potential for low-dose spine imaging according to recent simulation studies, particularly when used in combination with advanced iterative image reconstruction algorithms [36, 37].

Concerning the calculation of vBMD from vertebral bodies, the precision of standard manual placement of regions of interest (e. g., circle drawn in mid-sagittal planes of spine CT) for extraction of attenuation values followed by conversion into vBMD has been shown to be adequately precise [24]. While this approach may be justified under clinical conditions and time constraints, it does not cover the entire structural information of a vertebral body. More representative manual segmentation would be rather time-consuming. Hence, with the development of (semi)automated algorithms for vertebral body segmentation from CT data, segmentation of the entire vertebral bodies along the whole spine may be possible with reasonably low effort once the segmentation pipeline is implemented [18]. In this regard, an investigation using a deep-learning-based architecture for automated vertebral segmentation extracted measures in an opportunistic setup, reporting that they performed significantly better as predictors for VFs compared to DXA (area under the curve [AUC] = 0.885 for trabecular vBMD) [38]. Translation to clinical applicability is facilitated by freely available training and validation databases derived from deep-learning-based algorithms such as Anduin (https://anduin.bonescreen.de/) (▶ **Fig. 3, 4**) [39]. Notably, using this tool may also circumvent the issue of metal artifacts (e. g., due to previous spinal instrumentation) for vertebral vBMD measurements, given that automatically set thresholds could filter out biasing attenuation peaks (▶ **Fig. 4**) [40].

Moreover, advanced image analysis techniques such as TA and numerical engineering methods such as finite element analysis (FEA) are increasingly used to provide information about bone quality and strength beyond vBMD. Particularly when the spatial resolution of CT scans is not sufficient to depict every structural detail within a vertebral body, TA could provide relevant spatial and heterogeneity information of gray-level values in images. As such, TA reflects an objective and quantitative approach to analyze the distribution and relationship of pixel or voxel gray levels in CT images. Specifically, TA using CT data from the clinical routine made it possible to distinguish between patients with and without osteoporotic fractures [41]. On a similar note, texture parameters derived from standard CT exams combined with machine learning identified patients who would suffer from VFs with high accuracy (AUC = 0.97) [42].

Furthermore, FEA is suitable for relating morphological and material variations and properties to functional characteristics, thus enabling a reduction of complex geometries to a finite number of elements with simple geometries (▶ **Fig. 5, 6**). Specifically, the FEA method can provide realistic 3 D models of bone reconstructed from radiological image data and apply material properties to an FEA-meshed model (▶ **Fig. 5**) [18]. Then, boundary and loading conditions can be simulated to obtain structural, mechanical, and fracture characteristics to predict bone strength and individual fracture risk (▶ **Fig. 6**) [18]. Elastic modulus is an intrinsic material property and is not influenced by geometry, while bone geometry affects stress and deformation behavior. Considering that bone is a semi-brittle material, it will deform elastically up to the elastic (or yield) limit, followed by some yielding (exhibiting ductility) and, finally, collapsing at the ultimate stress. The Von-Mises stress is the stress component associated with the distortion energy of the bone when a mechanical load acts on the top surface. Thus, Von-Mises stress is used as a measurement metric to determine whether the structure has started to yield at any point (▶ **Fig. 6**). Of note, patient-specific image-based FEA reflects the current reference standard to estimate vertebral strength and has been shown to predict vertebral body compressive strength better than QCT-derived vBMD for an in-vitro scenario [43].

Additionally, for the in-vivo setup, lower vertebral strength derived from FEA was associated with an increased risk of new or worsening VFs, and vertebral strength better predicted incident VFs than CT-based aBMD (AUC = 0.804 vs. 0.715) [44]. Of note, instead of incorporating only FEA-based measurements from single or multiple vertebral bodies, a functional spinal unit (FSU) that consists of at least two adjacent vertebrae with the intervertebral disc could be considered (▶ **Fig. 5, 6**) [45]. As such, the FSU may represent a more realistic model than the isolated vertebral body to evaluate the actual load and its distribution [45]. However, regarding both TA and FEA, it must be acknowledged that extracted metrics have not been standardized yet, and normative values have not been developed either. Performing FEA also requires high computational power, effort, and technical exper-

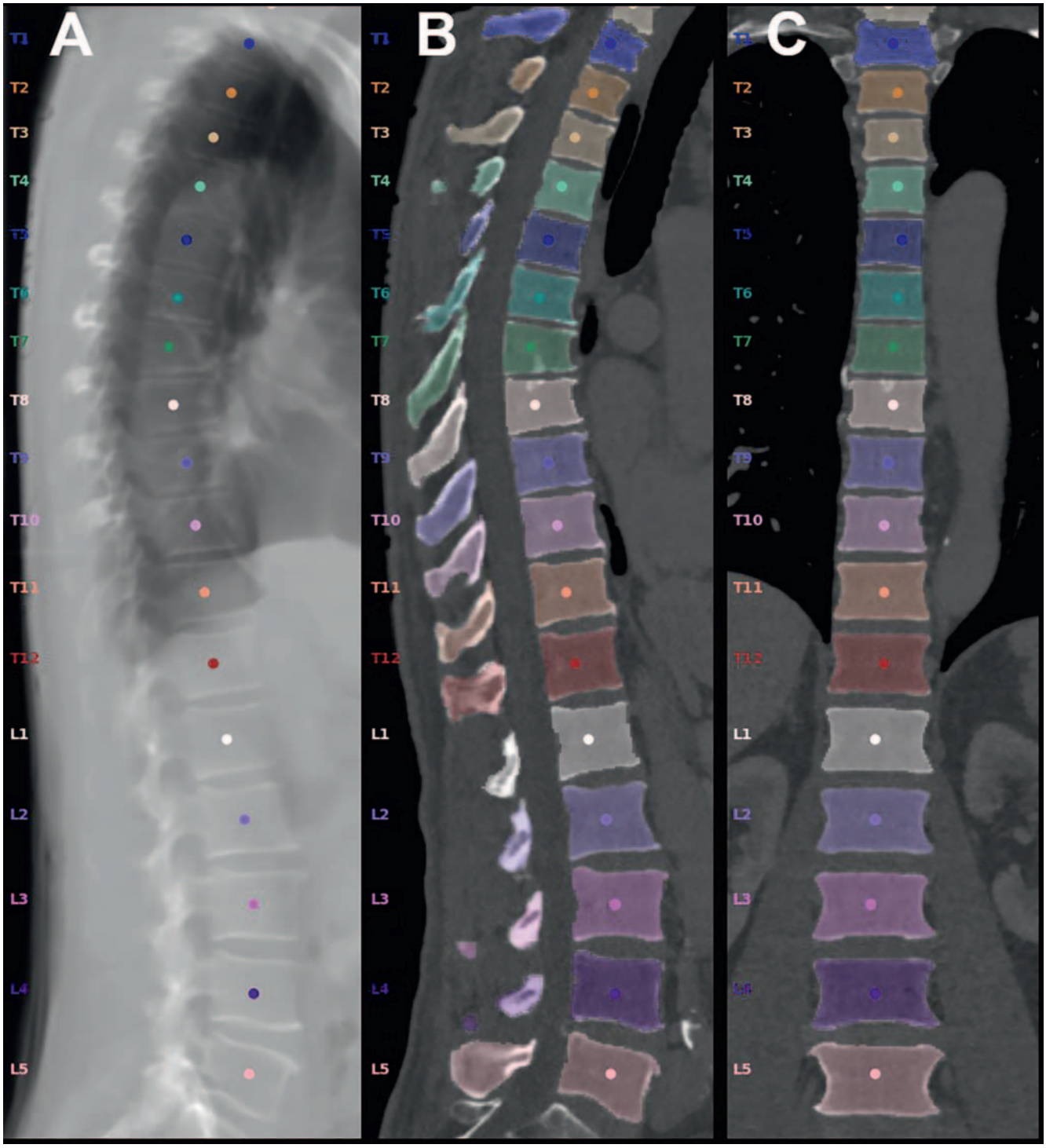

▶ **Fig. 3** Automated labeling and segmentation in routine computed tomography (CT) – generation of segmentation masks and virtual images. Labeling of vertebral bodies with segmentations using a deep-learning-based algorithm based on multi-detector CT data acquired in the clinical routine, enabling automated application for opportunistic osteoporosis assessment. **A** Virtual radiograph in lateral projection as generated from CT input data; **B** automated labeling and segmentation of vertebral bodies (T1-L5) in sagittal view; **C** automated labeling and segmentation of vertebral bodies (T1-L5) in coronal view.

tise, often hampering clinical usability and approaches that aim for FEA of more than a few preselected vertebrae.

Magnetic resonance imaging

Principles and main findings

A multitude of MRI techniques can be leveraged to study bone microstructure and bone marrow (BM), starting with T2* mapping

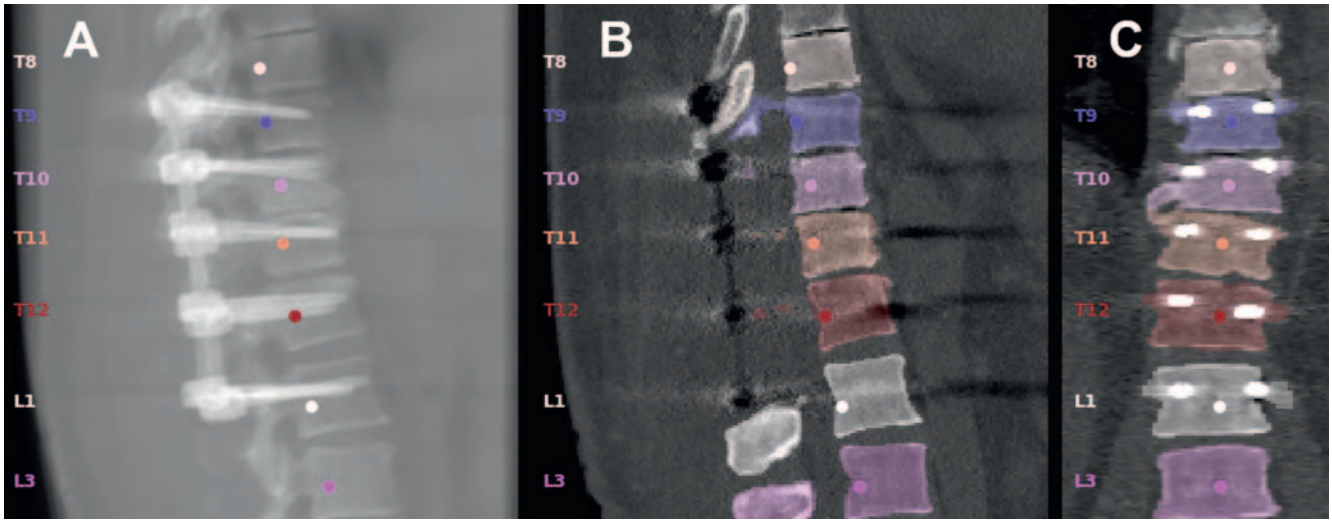

▶ **Fig. 4** Automated labeling and segmentation in routine computed tomography (CT) – spinal instrumentation. Labeling of vertebral bodies with segmentations in routine multi-detector CT data using a deep-learning-based algorithm in the presence of metal implants (dorsal stabilization T9-L1). **A** Virtual radiograph in lateral projection as generated from CT input data; **B** automated labeling and segmentation of vertebral bodies (T8-L3) in sagittal view (with segmentation masks not including the screws and only reaching to the screw contours); **C** automated labeling and segmentation of vertebral bodies (T8-L3) in coronal view (with segmentation masks not including the screws and only reaching to the screw contours).

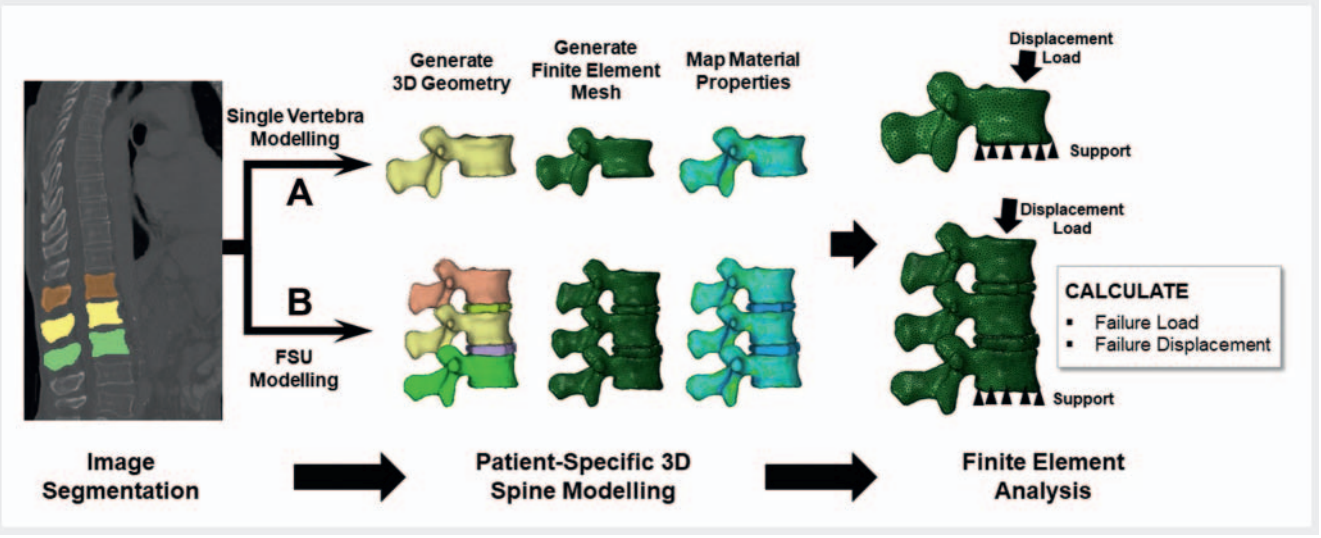

▶ **Fig. 5** Schematic illustration of the workflow for finite element analysis (FEA) of three-dimensional (3D) single vertebrae and functional spinal unit (FSU) models for calculating failure load and displacement. The vertebral bodies (and intervertebral discs) are segmented from computed tomography (CT) image data, and 3D models are generated, which are meshed with tetrahedral elements. Subsequently, material properties, using empirical relations with respect to Hounsfield units (HU), are mapped to the mesh and boundary and loading conditions are applied before proceeding with the analysis. The model is then solved, and the parameters (failure load and failure displacement) are extracted. **A** FEA for a single vertebral body; **B** FEA for an FSU consisting of three vertebral bodies and adjacent intervertebral discs.

and high-resolution trabecular bone imaging introduced in the 1990 s [46–48]. In addition, since the 2000 s, magnetic resonance spectroscopy (MRS) and particularly chemical shift encoding-based water-fat MRI (CSE-MRI) are two techniques widely used for quantitative MRI of BM in the evaluation of osteoporosis (▶ **Fig. 7**) [46]. These techniques enable fat quantification of BM to extract the BM fat fraction (BMFF) or the proton density fat fraction (PDFF) as a fundamental tissue property that is calculated as the ratio of the density of mobile protons from fat (triglycerides) and the total density of protons from mobile triglycerides and mobile water (▶ **Fig. 7**) [49].

Using MRS, significantly increased vertebral BMFF in osteoporotic subjects has been revealed consistently, accompanied by an inverse correlation of vertebral BMFF with QCT-derived vBMD as well as DXA-derived aBMD or respective T-scores (exemplary range of reported correlation coefficients: $r = -0.20$ to -0.45) [50–52]. Furthermore, this inverse correlation has been extended to biomechanical properties by in-vitro testing, revealing negative

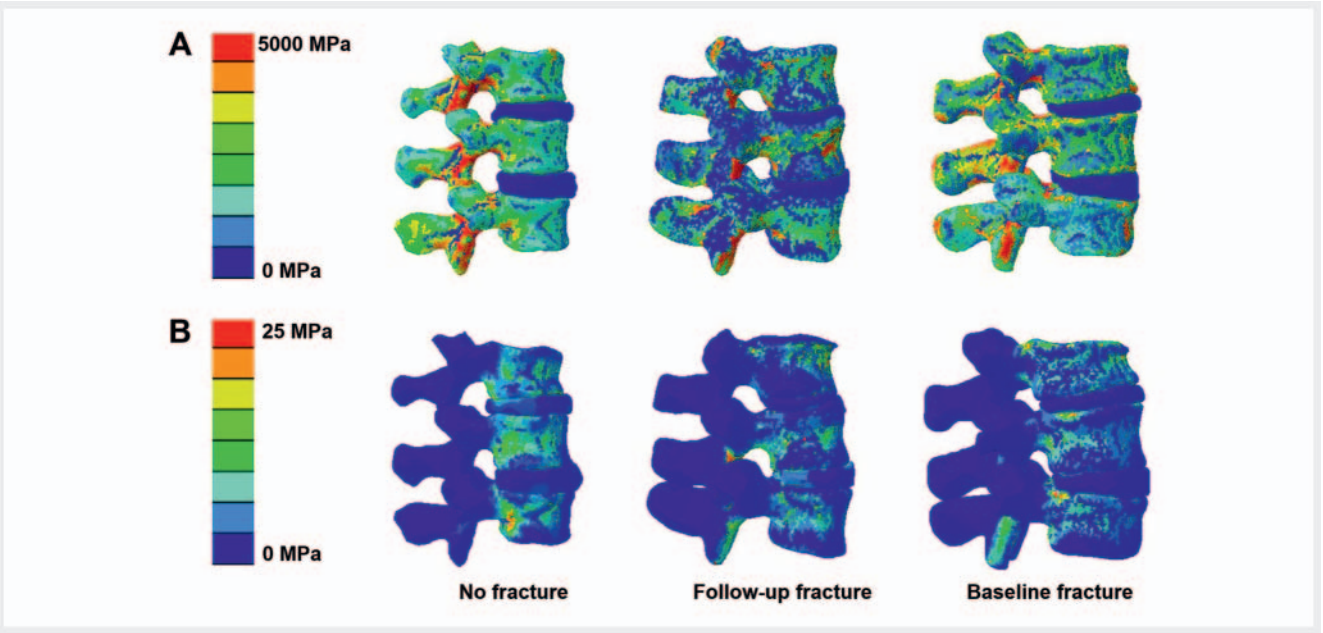

▶ **Fig. 6** Representative images of elastic modulus distribution and Von-Mises stress distribution derived from finite element analysis (FEA) for a functional spinal unit (FSU). Distributions are shown for a case without a vertebral fracture, a case with one baseline fracture (sustained fracture at the time point of imaging), and for one case that would show a fracture during later follow-up imaging (increased risk for fracture). Elastic modulus is derived from applying empirical equations to the Hounsfield units (HU) derived from the underlying computed tomography (CT) images, representing a quantity to measure an object's resistance to being deformed elastically under mechanical stress conditions. Von-Mises stress is a quantitative measure used to determine if a given object will yield or fracture. **A** Elastic modulus distribution; **B** Von-Mises stress distribution for an FSU consisting of three vertebral bodies and adjacent intervertebral discs. MPa: Megapascal Pressure Unit.

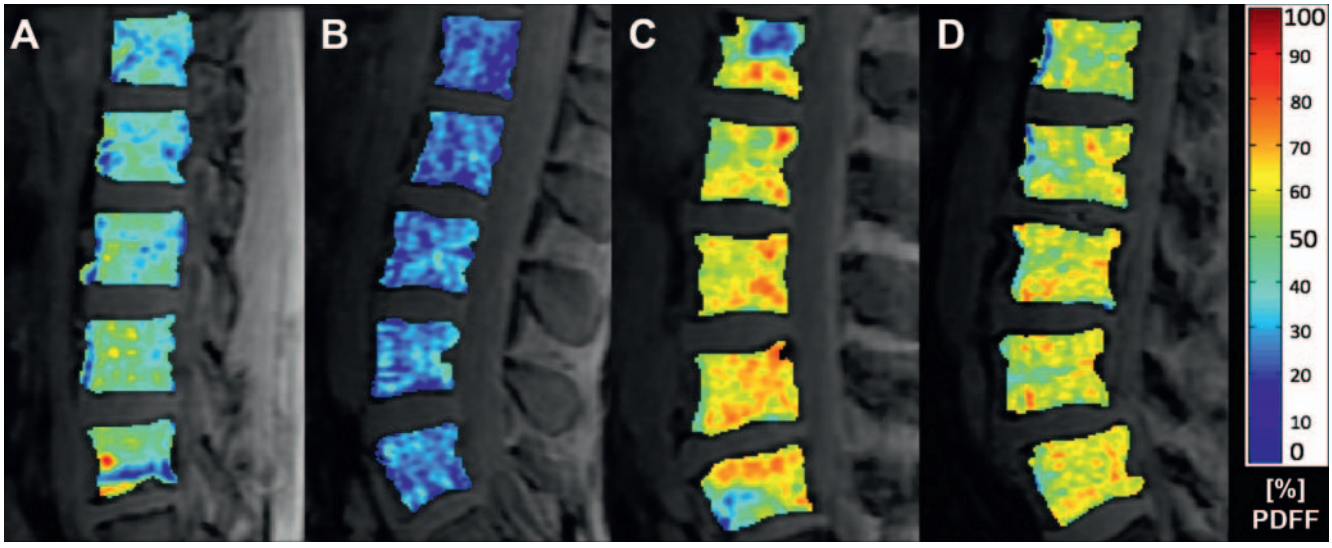

▶ **Fig. 7** Chemical shift encoding-based water-fat magnetic resonance imaging (CSE-MRI). Level-wise quantification of fat from vertebral bone marrow (BM) by CSE-MRI-derived proton density fat fraction (PDFF) for the lumbar spine (L1-L5) in a 31-year-old male **A**, 30-year old female **B**, 66-year-old female **C**, and 63-year-old male **D**. There is an increase in the PDFF with age for both sexes. Furthermore, the premenopausal woman **B** has lower vertebral PDFF compared to the man of similar age **A**, while this condition is reversed after menopause with higher vertebral PDFF for the female patient **C** compared to the male patient of a similar age **D**. Osteoporosis is typically characterized by increased vertebral PDFF. In this context, the PDFF is calculated as the ratio of the density of mobile protons from fat (triglycerides) and the total density of protons from mobile triglycerides and mobile water and is given in % (low PDFF shown in blue, high PDFF shown in red color).

correlations between vertebral failure loads and BMFF [53]. Regarding fracture status, males with VFs showed significantly increased vertebral BMFF [52].

For CSE-MRI, strong correlations with MRS-based BMFF quantification have been reported for the spine (exemplary range of reported correlation coefficients: r = 0.78–0.98) [54, 55]. Comparable

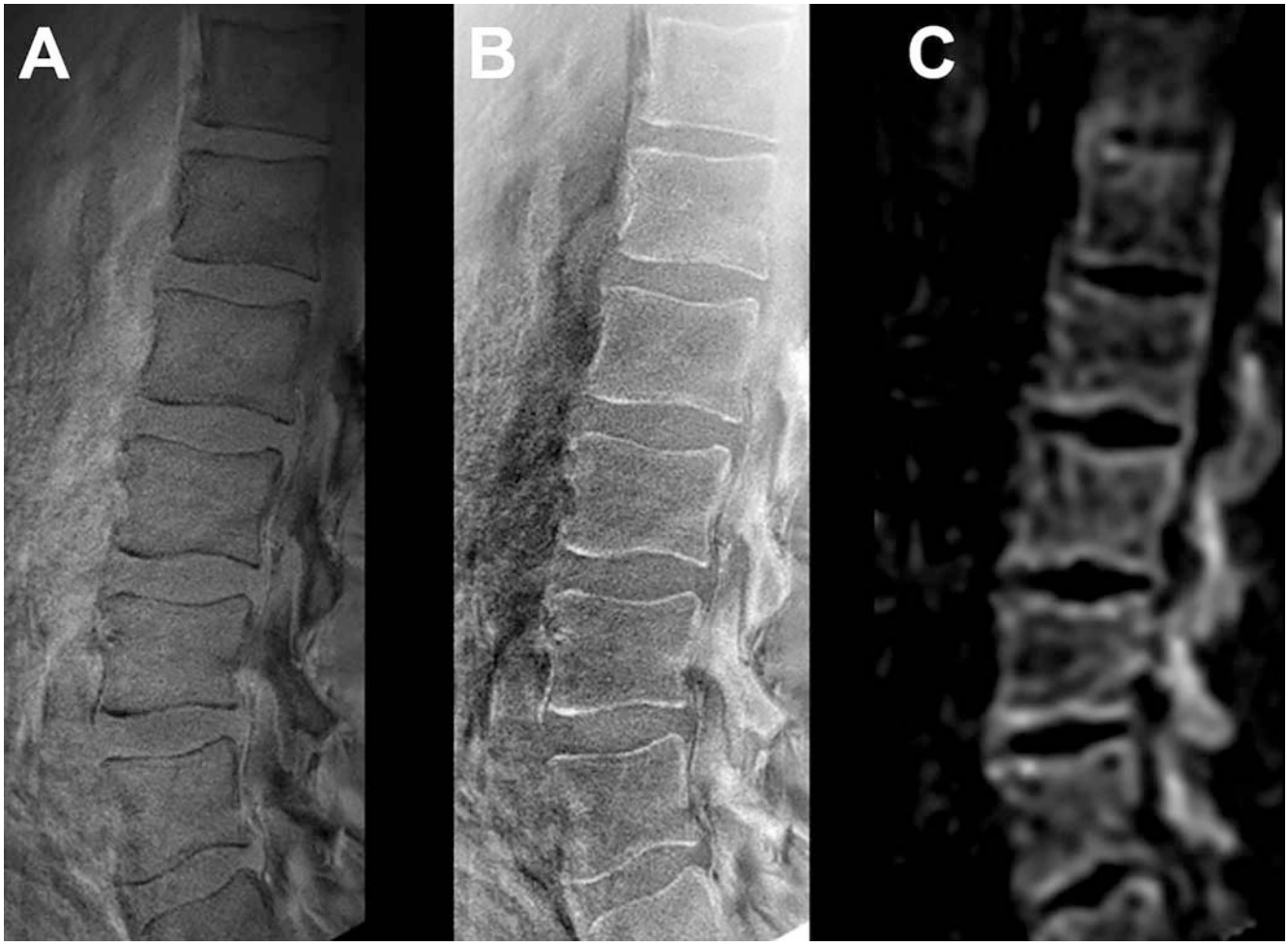

▶ **Fig. 8** Ultra-short echo time (UTE) imaging. Imaging of the lower spine of a 29-year-old male with a high-resolution (voxel size: 0.45 mm × 0.45 mm × 3 mm) UTE stack-of-stars sequence. The UTE image was T2*-weighted, T1-weighted, and proton density-weighted **A**. Due to the small flip angle of 5°, the contrast was mainly driven by the proton density. Cortical bone was highlighted by inverting the image contrast such that bone appeared bright **B**. A three-dimensional (3 D) inversion recovery (IR)-prepared UTE sequence with the same field of view, but with lower resolution (voxel size: 3 mm isotropic) is additionally displayed **C**. Long T2 components such as present for fat and muscle were suppressed, while tissues with short T2* appeared bright (cortical bone, trabecular bone, ligaments, and tendons). Using UTE with these methods could enable selective bone visualization and quantitative assessment of short T2 water components in vivo.

to the results of MRS, BMFF derived from CSE-MRI was elevated in subjects with osteoporosis and inversely associated with vBMD values from QCT [54, 56, 57]. Notably, PDFF extracted from CSE-MRI enabled the differentiation between osteoporotic and malignant VFs, with vertebral PDFF showing significantly lower values in malignant compared to acute osteoporotic fractures [58]. Given these promising results, PDFF, as derived from MRS or CSE-MRI, has the potential to become a viable in-vivo surrogate biomarker of bone health.

Perspectives and novel analysis approaches

Besides MRS and CSE-MRI, other MRI methods such as quantitative susceptibility mapping (QSM) for imaging of trabecular bone and ultra-short echo time (UTE) for imaging of cortical bone have been developed and applied to the spine [46]. Methodologically closely related to T2*, QSM has been introduced as a more direct measure of susceptibility differences between trabecularized BM and surrounding tissues. Initial studies using QSM for the spine demonstrated significantly increased vertebral magnetic susceptibility in osteopenia and osteoporosis, with a sensitivity/specificity for differentiating osteoporosis from non-osteoporosis of 80.8 %/77.3 % [59, 60]. However, these studies did not implement chemical shift encoding-based water-fat separation for field map generation. Thus, the results should be primarily interpreted qualitatively until further confirmation is achieved.

Another approach is the direct measurement of the bone matrix signal, which can be achieved with UTE imaging (▶ **Fig. 8**). While the direct detection of the bone tissue signal is nearly impossible for conventional MRI due to rapid signal decay, sampling at a UTE of 30–200 µs combined with suppression of long-T2 tissues could allow direct visualization with sufficient contrast [46]. To date, UTE imaging has allowed cortical bone porosity assessment ex-vivo and pore water concentration mapping in-vivo at the tibia, suggesting clinical usefulness [61, 62]. However, despite the merit of direct bone visualization, UTE imaging for the evalua-

tion of osteoporosis of the spine has only been recently proposed [63]. Specifically, one study showed that bound water proton density mapping can be achieved in the spine by comparing its signal obtained from 3 D inversion recovery UTE imaging and that of an external reference phantom with known proton density [63].

In contrast to DXA and CT, MRI is a radiation-free technique, and assessment of vertebral BMFF is possible without contrast medium injection. Consequently, scanning for research purposes and with large spatial coverage could be achieved without safety issues. Thus, fat quantification along the entire spine could be achieved, allowing exploration of BMFF variations. For instance, CSE-MRI revealed a spatial pattern of BMFF increase in the cranio-caudal direction along the spine [64]. Furthermore, significant relations between vertebral BMFF and fat content of paraspinal muscles were observed in postmenopausal women, potentially providing MRI-based evidence for systemic fat compartment alterations in osteoporosis [65]. Another approach to investigate region-specific patterns of vertebral BMFF is TA, which revealed increased vertebral BMFF heterogeneity in postmenopausal women, and, specifically, the second-order features Contrast and Dissimilarity allowed differentiation between pre- and postmenopausal women equally well compared to PDFF [66]. Furthermore, by means of TA based on CSE-MRI data, it has been shown that vertebral BMFF heterogeneity is primarily dependent on sex and age, which can have implications for osteoporosis screening particularly in elderly women [67].

Conclusion

Quantitative 3 D imaging is playing an increasing role in osteoporosis diagnostics and VF risk evaluation. The reference standard remains the 2 D measurement of aBMD by DXA, but many CT- and MRI-based techniques have been developed to shed light on various aspects of bone quality, structure, and strength. In addition, the 3 D nature of data provided by CT and MRI may be most efficiently used when paired with advanced analysis techniques (e. g., TA, FEA, and automated segmentation algorithms) to further improve fracture prediction beyond aBMD, and to provide spatially resolved investigations of vertebral body surface and microstructure. However, without developing distinct and experimentally validated diagnostic criteria for osteoporosis based on CT- and MRI-derived measures, novel approaches cannot yet undergo a broad transition to the clinical routine.

Funding

German Society of Musculoskeletal Radiology; B. Braun Foundation (BBST-D-19–00 106); Dr.-Ing. Leonhard Lorenz Foundation (968/19); Deutsche Forschungsgemeinschaft (432 290 010); H2020 European Research Council (637 164 – iBack)

Conflict of Interest

The authors declare that they have no conflict of interest.

References

[1] NIH Consensus Development Panel on Osteoporosis Prevention Diagnosis and Therapy. Osteoporosis prevention, diagnosis, and therapy. Jama 2001; 285: 785–795

[2] Hallberg I, Bachrach-Lindstrom M, Hammerby S et al. Health-related quality of life after vertebral or hip fracture: a seven-year follow-up study. BMC Musculoskelet Disord 2009; 10: 135. doi:10.1186/1471-2474-10-135

[3] Bliuc D, Nguyen ND, Milch VE et al. Mortality risk associated with low-trauma osteoporotic fracture and subsequent fracture in men and women. Jama 2009; 301: 513–521. doi:10.1001/jama.2009.50

[4] Melton LJ 3rd, Atkinson EJ, Cooper C et al. Vertebral fractures predict subsequent fractures. Osteoporos Int 1999; 10: 214–221

[5] Arabi A, Baddoura R, Awada H et al. Discriminative ability of dual-energy X-ray absorptiometry site selection in identifying patients with osteoporotic fractures. Bone 2007; 40: 1060–1065. doi:10.1016/j.bone.2006.11.017

[6] Maricic M. Use of DXA-based technology for detection and assessment of risk of vertebral fracture in rheumatology practice. Curr Rheumatol Rep 2014; 16: 436. doi:10.1007/s11926-014-0436-5

[7] Siris ES, Chen YT, Abbott TA et al. Bone mineral density thresholds for pharmacological intervention to prevent fractures. Archives of internal medicine 2004; 164: 1108–1112. doi:10.1001/archinte.164.10.1108

[8] World Health Organization. Assessment of fracture risk and its application to screening for postmenopausal osteoporosis. Report of a WHO Study Group. World Health Organ Tech Rep Ser 1994; 843: 1–129

[9] Yu W, Gluer CC, Fuerst T et al. Influence of degenerative joint disease on spinal bone mineral measurements in postmenopausal women. Calcif Tissue Int 1995; 57: 169–174

[10] Bolotin HH. DXA in vivo BMD methodology: an erroneous and misleading research and clinical gauge of bone mineral status, bone fragility, and bone remodelling. Bone 2007; 41: 138–154. doi:10.1016/j.bone.2007.02.022

[11] Promma S, Sritara C, Wipuchwongsakorn S et al. Errors in Patient Positioning for Bone Mineral Density Assessment by Dual X-Ray Absorptiometry: Effect of Technologist Retraining. J Clin Densitom 2018; 21: 252–259. doi:10.1016/j.jocd.2017.07.004

[12] World Health Organization. Assessment of osteoporosis at the primary health care level. Summary Report of a WHO Scientific Group. Geneva: WHO. 2007

[13] Hans D, Goertzen AL, Krieg MA et al. Bone microarchitecture assessed by TBS predicts osteoporotic fractures independent of bone density: the Manitoba study. J Bone Miner Res 2011; 26: 2762–2769. doi:10.1002/jbmr.499

[14] Boutroy S, Hans D, Sornay-Rendu E et al. Trabecular bone score improves fracture risk prediction in non-osteoporotic women: the OFELY study. Osteoporos Int 2013; 24: 77–85. doi:10.1007/s00198-012-2188-2

[15] Kanis JA, Johnell O, Oden A et al. FRAX and the assessment of fracture probability in men and women from the UK. Osteoporos Int 2008; 19: 385–397. doi:10.1007/s00198-007-0543-5

[16] American College of Radiology (2018) ACR–SPR–SSR practice parameter for the performance of musculoskeletal quantitative computed tomography (QCT). American College of Radiology, Reston. Available via (Accessed 7 June 2021) https://www.acr.org/-/media/ACR/Files/Practice-Parameters/QCT.pdf?la

[17] Oftadeh R, Perez-Viloria M, Villa-Camacho JC et al. Biomechanics and mechanobiology of trabecular bone: a review. J Biomech Eng 2015; 137. doi:10.1115/1.4029176

[18] Loffler MT, Sollmann N, Mei K et al. X-ray-based quantitative osteoporosis imaging at the spine. Osteoporos Int 2019. doi:10.1007/s00198-019-05212-2

[19] Link TM, Kazakia G. Update on Imaging-Based Measurement of Bone Mineral Density and Quality. Curr Rheumatol Rep 2020; 22: 13. doi:10.1007/s11926-020-00892-w

[20] Pfeilschifter J, Diel IJ. Osteoporosis due to cancer treatment: pathogenesis and management. Journal of clinical oncology: official journal of the American Society of Clinical Oncology 2000; 18: 1570–1593. doi:10.1200/JCO.2000.18.7.1570

[21] Hopper KD, Wang MP, Kunselman AR. The use of clinical CT for baseline bone density assessment. Journal of computer assisted tomography 2000; 24: 896–899. doi:10.1097/00004728-200011000-00015

[22] Link TM, Koppers BB, Licht T et al. In vitro and in vivo spiral CT to determine bone mineral density: initial experience in patients at risk for osteoporosis. Radiology 2004; 231: 805–811. doi:10.1148/radiol.2313030325

[23] Bauer JS, Henning TD, Mueller D et al. Volumetric quantitative CT of the spine and hip derived from contrast-enhanced MDCT: conversion factors. Am J Roentgenol American journal of roentgenology 2007; 188: 1294–1301. doi:10.2214/Am J Roentgenol.06.1006

[24] Baum T, Muller D, Dobritz M et al. BMD measurements of the spine derived from sagittal reformations of contrast-enhanced MDCT without dedicated software. Eur J Radiol 2011; 80: e140–e145. doi:10.1016/j.ejrad.2010.08.034

[25] Baum T, Muller D, Dobritz M et al. Converted lumbar BMD values derived from sagittal reformations of contrast-enhanced MDCT predict incidental osteoporotic vertebral fractures. Calcif Tissue Int 2012; 90: 481–487. doi:10.1007/s00223-012-9596-3

[26] Pickhardt PJ, Lee LJ, del Rio AM et al. Simultaneous screening for osteoporosis at CT colonography: bone mineral density assessment using MDCT attenuation techniques compared with the DXA reference standard. J Bone Miner Res 2011; 26: 2194–2203. doi:10.1002/jbmr.428

[27] Weaver AA, Beavers KM, Hightower RC et al. Lumbar Bone Mineral Density Phantomless Computed Tomography Measurements and Correlation with Age and Fracture Incidence. Traffic Inj Prev 2015; 16 (Suppl. 2): S153–S160. doi:10.1080/15389588.2015.1054029

[28] McCarthy I. The physiology of bone blood flow: a review. The Journal of bone and joint surgery American volume 2006; 88 (Suppl. 3): 4–9. doi:10.2106/JBJS.F.00890

[29] Toelly A, Bardach C, Weber M et al. Influence of Contrast Media on Bone Mineral Density (BMD) Measurements from Routine Contrast-Enhanced MDCT Datasets using a Phantom-less BMD Measurement Tool. Fortschr Röntgenstr 2017; 189: 537–543. doi:10.1055/s-0043-102941

[30] Abdullayev N, Neuhaus VF, Bratke G et al. Effects of Contrast Enhancement on In-Body Calibrated Phantomless Bone Mineral Density Measurements in Computed Tomography. J Clin Densitom 2018; 21: 360–366. doi:10.1016/j.jocd.2017.10.001

[31] Damilakis J, Adams JE, Guglielmi G et al. Radiation exposure in X-ray-based imaging techniques used in osteoporosis. European radiology 2010; 20: 2707–2714. doi:10.1007/s00330-010-1845-0

[32] Mei K, Schwaiger BJ, Kopp FK et al. Bone mineral density measurements in vertebral specimens and phantoms using dual-layer spectral computed tomography. Sci Rep 2017; 7: 17519. doi:10.1038/s41598-017-17855-4

[33] van Hamersvelt RW, Schilham AMR, Engelke K et al. Accuracy of bone mineral density quantification using dual-layer spectral detector CT: a phantom study. European radiology 2017; 27: 4351–4359. doi:10.1007/s00330-017-4801-4

[34] Roski F, Hammel J, Mei K et al. Bone mineral density measurements derived from dual-layer spectral CT enable opportunistic screening for osteoporosis. European radiology 2019; 29: 6355–6363. doi:10.1007/s00330-019-06263-z

[35] Roski F, Hammel J, Mei K et al. Opportunistic osteoporosis screening: contrast-enhanced dual-layer spectral CT provides accurate measurements of vertebral bone mineral density. European radiology 2021; 31: 3147–3155. doi:10.1007/s00330-020-07319-1

[36] Sollmann N, Mei K, Riederer I et al. Low-dose MDCT: evaluation of the impact of systematic tube current reduction and sparse sampling on the detection of degenerative spine diseases. European radiology 2021; 31: 2590–2600. doi:10.1007/s00330-020-07278-7

[37] Sollmann N, Mei K, Hedderich DM et al. Multi-detector CT imaging: impact of virtual tube current reduction and sparse sampling on detection of vertebral fractures. European radiology 2019; 29: 3606–3616. doi:10.1007/s00330-019-06090-2

[38] Loffler MT, Jacob A, Scharr A et al. Automatic opportunistic osteoporosis screening in routine CT: improved prediction of patients with prevalent vertebral fractures compared to DXA. European radiology 2021. doi:10.1007/s00330-020-07655-2

[39] Loffler MT, Sekuboyina A, Jacob A et al. A Vertebral Segmentation Dataset with Fracture Grading. Radiol Artif Intell 2020; 2: e190138. doi:10.1148/ryai.2020190138

[40] Loffler MT, Sollmann N, Burian E et al. Opportunistic Osteoporosis Screening Reveals Low Bone Density in Patients With Screw Loosening After Lumbar Semi-Rigid Instrumentation: A Case-Control Study. Front Endocrinol (Lausanne) 2020; 11: 552719. doi:10.3389/fendo.2020.552719

[41] Mookiah MRK, Rohrmeier A, Dieckmeyer M et al. Feasibility of opportunistic osteoporosis screening in routine contrast-enhanced multi detector computed tomography (MDCT) using texture analysis. Osteoporos Int 2018; 29: 825–835. doi:10.1007/s00198-017-4342-3

[42] Muehlematter UJ, Mannil M, Becker AS et al. Vertebral body insufficiency fractures: detection of vertebrae at risk on standard CT images using texture analysis and machine learning. European radiology 2019; 29: 2207–2217. doi:10.1007/s00330-018-5846-8

[43] Crawford RP, Cann CE, Keaveny TM. Finite element models predict in vitro vertebral body compressive strength better than quantitative computed tomography. Bone 2003; 33: 744–750. doi:10.1016/s8756-3282(03)00210-2

[44] Allaire BT, Lu D, Johannesdottir F et al. Prediction of incident vertebral fracture using CT-based finite element analysis. Osteoporos Int 2019; 30: 323–331. doi:10.1007/s00198-018-4716-1

[45] Anitha DP, Baum T, Kirschke JS et al. Effect of the intervertebral disc on vertebral bone strength prediction: a finite-element study. Spine J 2020; 20: 665–671. doi:10.1016/j.spinee.2019.11.015

[46] Sollmann N, Loffler MT, Kronthaler S et al. MRI-Based Quantitative Osteoporosis Imaging at the Spine and Femur. Journal of magnetic resonance imaging: JMRI 2020. doi:10.1002/jmri.27260

[47] Majumdar S, Thomasson D, Shimakawa A et al. Quantitation of the susceptibility difference between trabecular bone and bone marrow: experimental studies. Magnetic resonance in medicine: official journal of the Society of Magnetic Resonance in Medicine/Society of Magnetic Resonance in Medicine 1991; 22: 111–127. doi:10.1002/mrm.1910220112

[48] Wehrli FW, Ford JC, Attie M et al. Trabecular structure: preliminary application of MR interferometry. Radiology 1991; 179: 615–621. doi:10.1148/radiology.179.3.2027962

[49] Reeder SB, Hu HH, Sirlin CB. Proton density fat-fraction: a standardized MR-based biomarker of tissue fat concentration. Journal of magnetic resonance imaging: JMRI 2012; 36: 1011–1014. doi:10.1002/jmri.23741

[50] Griffith JF, Yeung DK, Antonio GE et al. Vertebral bone mineral density, marrow perfusion, and fat content in healthy men and men with osteoporosis: dynamic contrast-enhanced MR imaging and MR spectroscopy. Radiology 2005; 236: 945–951. doi:10.1148/radiol.2363041425

[51] Baum T, Yap SP, Karampinos DC et al. Does vertebral bone marrow fat content correlate with abdominal adipose tissue, lumbar spine bone mineral density, and blood biomarkers in women with type 2 diabetes mellitus? Journal of magnetic resonance imaging: JMRI 2012; 35: 117–124. doi:10.1002/jmri.22757

[52] Schwartz AV, Sigurdsson S, Hue TF et al. Vertebral bone marrow fat associated with lower trabecular BMD and prevalent vertebral fracture in older adults. J Clin Endocrinol Metab 2013; 98: 2294–2300. doi:10.1210/jc.2012-3949

[53] Karampinos DC, Ruschke S, Gordijenko O et al. Association of MRS-Based Vertebral Bone Marrow Fat Fraction with Bone Strength in a Human In Vitro Model. J Osteoporos 2015; 2015: 152349. doi:10.1155/2015/152349

[54] Li G, Xu Z, Gu H et al. Comparison of chemical shift-encoded water-fat MRI and MR spectroscopy in quantification of marrow fat in postmenopausal females. Journal of magnetic resonance imaging: JMRI 2017; 45: 66–73. doi:10.1002/jmri.25351

[55] Shen W, Gong X, Weiss J et al. Comparison among T1-weighted magnetic resonance imaging, modified dixon method, and magnetic resonance spectroscopy in measuring bone marrow fat. J Obes 2013; 2013: 298675. doi:10.1155/2013/298675

[56] Kuhn JP, Hernando D, Meffert PJ et al. Proton-density fat fraction and simultaneous R2* estimation as an MRI tool for assessment of osteoporosis. European radiology 2013; 23: 3432–3439. doi:10.1007/s00330-013-2950-7

[57] Zhao Y, Huang M, Ding J et al. Prediction of Abnormal Bone Density and Osteoporosis From Lumbar Spine MR Using Modified Dixon Quant in 257 Subjects With Quantitative Computed Tomography as Reference. Journal of magnetic resonance imaging: JMRI 2019; 49: 390–399. doi:10.1002/jmri.26233

[58] Schmeel FC, Luetkens JA, Enkirch SJ et al. Proton density fat fraction (PDFF) MR imaging for differentiation of acute benign and neoplastic compression fractures of the spine. European radiology 2018; 28: 5001–5009. doi:10.1007/s00330-018-5513-0

[59] Chen Y, Guo Y, Zhang X et al. Bone susceptibility mapping with MRI is an alternative and reliable biomarker of osteoporosis in postmenopausal women. European radiology 2018; 28: 5027–5034. doi:10.1007/s00330-018-5419-x

[60] Guo Y, Chen Y, Zhang X et al. Magnetic Susceptibility and Fat Content in the Lumbar Spine of Postmenopausal Women With Varying Bone Mineral Density. Journal of magnetic resonance imaging: JMRI 2018. doi:10.1002/jmri.26279

[61] Manhard MK, Harkins KD, Gochberg DF et al. 30-Second bound and pore water concentration mapping of cortical bone using 2D UTE with optimized half-pulses. Magnetic resonance in medicine: official journal of the Society of Magnetic Resonance in Medicine/Society of Magnetic Resonance in Medicine 2017; 77: 945–950. doi:10.1002/mrm.26605

[62] Rajapakse CS, Bashoor-Zadeh M, Li C et al. Volumetric Cortical Bone Porosity Assessment with MR Imaging: Validation and Clinical Feasibility. Radiology 2015; 276: 526–535. doi:10.1148/radiol.15141850

[63] Ma YJ, Chen Y, Li L et al. Trabecular bone imaging using a 3D adiabatic inversion recovery prepared ultrashort TE Cones sequence at 3T. Magnetic resonance in medicine: official journal of the Society of Magnetic Resonance in Medicine/Society of Magnetic Resonance in Medicine 2020; 83: 1640–1651. doi:10.1002/mrm.28027

[64] Baum T, Rohrmeier A, Syvari J et al. Anatomical Variation of Age-Related Changes in Vertebral Bone Marrow Composition Using Chemical Shift Encoding-Based Water-Fat Magnetic Resonance Imaging. Front Endocrinol (Lausanne) 2018; 9: 141. doi:10.3389/fendo.2018.00141

[65] Sollmann N, Dieckmeyer M, Schlaeger S et al. Associations Between Lumbar Vertebral Bone Marrow and Paraspinal Muscle Fat Compositions-An Investigation by Chemical Shift Encoding-Based Water-Fat MRI. Front Endocrinol (Lausanne) 2018; 9: 563. doi:10.3389/fendo.2018.00563

[66] Burian E, Subburaj K, Mookiah MRK et al. Texture analysis of vertebral bone marrow using chemical shift encoding-based water-fat MRI: a feasibility study. Osteoporos Int 2019; 30: 1265–1274. doi:10.1007/s00198-019-04924-9

[67] Dieckmeyer M, Junker D, Ruschke S et al. Vertebral Bone Marrow Heterogeneity Using Texture Analysis of Chemical Shift Encoding-Based MRI: Variations in Age, Sex, and Anatomical Location. Front Endocrinol (Lausanne) 2020; 11: 555931. doi:10.3389/fendo.2020.555931